Oxygen hole symmetry and banding in cuprate superconductors

L. F. Mattheiss and D. R. Hamann
AT&T Bell Laboratories, Murray Hill, New Jersey 07974
(Received 6 March 1989)

A simple procedure is proposed for modeling the O $2p$ bands of cuprate compounds in the limit where the Cu $3d$ electrons are localized by correlation effects such as the on-site Coulomb energy U_d. This scheme, which involves orthogonalization of the linear augmented-plane-wave (LAPW) basis to the Cu $3d$ states, has been applied to $Ca_{0.86}Sr_{0.14}CuO_2$, the parent compound of the Bi-Sr-Ca-Cu-O and Tl-Ba-Ca-Cu-O high-T_c superconductors. Tight-binding fits to the LAPW results for $Ca_{0.86}Sr_{0.14}CuO_2$ with localized and itinerant Cu $3d$ electrons yield O p-p interaction parameters which describe both limits equally well. According to this model, the doping-induced holes in the O $2p$ manifold depopulate initially bands containing σ-antibonding $p(x,y)$ orbitals that are pointed along the O—Cu bond directions, with π-antibonding $p(x,y)$ and $p(z)$ subbands entering only at larger hole concentrations.

Since the discovery of high-temperature superconductivity in the La-Ba-Cu-O system,[1] there has been an enormous theoretical and experimental effort to elucidate the electronic properties of this ever-growing family of cuprate superconductors and parent compounds. The earliest insight was provided by the results of band-structure calculations[2,3] for La_2CuO_4, the parent compound of the Ba-doped $La_{2-x}Ba_xCuO_4$ superconductor. These calculations, carried out in the local-density approximation (LDA), predicted that La_2CuO_4 should exhibit metallic properties, resulting from a single half-filled Cu $d(x^2-y^2)$–O $p(x,y)$ σ-antibonding subband at E_F. The failure of subsequent local-spin-density calculations[4] to account for the observed insulating and antiferromagnetic properties[5] of La_2CuO_4 raised doubts concerning the adequacy of LDA results for describing the electronic properties of these cuprates. Additional discrepancies between the calculated LDA valence-band density of states (DOS) and that inferred from a variety of spectroscopic studies[6] on pure and Ba-doped La_2CuO_4 (as well as subsequent cuprates) provided added support for Anderson's early proposal[7] that on-site Coulomb interactions are crucial for determining the electronic properties of these cuprate superconductors.

Emery[8] was the first to propose that the extra holes introduced into the CuO_2 planes of La_2CuO_4 by Ba or Sr doping reside primarily within the O $2p$ bands as a result of electron-electron interactions. Assuming an extended three-band Hubbard model involving the Cu $d(x^2-y^2)$ and σ-bonding O $p(x,y)$ orbitals and approximate model parameters estimated from LDA results,[2,3] Emery proposed a model representation of the cuprate electronic properties which is illustrated schematically in Fig. 1.

According to this model, the Cu $3d$ on-site Coulomb energy U_d causes the LDA hybridized Cu $3d$–O $2p$ manifold to split into a filled lower Cu $3d$[9] Hubbard subband and an unfilled upper state, with intermediate O $2p$ bands. These O $2p$ bands fall within the Hubbard d gap provided that $U_d > \epsilon$, the O $2p$–Cu $3d$ orbital-energy difference. The extra holes introduced by Ba or Sr doping reduce the filling of the O $2p$ manifold, thereby producing metallic behavior as well as high-temperature superconductivity.

A variety of theoretical models have been proposed[9–14] which specify the detailed symmetry of the O $2p$ holes within this p-band complex that originates from the CuO_2 planes. These have been derived either from first-principles quantum-chemical calculations on Cu—O clusters (including short-range correlation effects) or various combinations of theoretical and experimental results. These proposals span the three possible orientations of these O $2p$ orbitals, which include the $\sigma(x,y)$,[9,14] $\pi(x,y)$,[10–12] and $\pi(z)$ (Ref. 13) states. In this notation, $\sigma(x,y)$ denotes O $2p$ orbitals that are pointed along the nearest-neighbor Cu—O bond directions and form σ-type bonds with the Cu $d(x^2-y^2)$ states. The $\pi(x,y)$ and $\pi(z)$ states are perpendicular to these and form π-type bonds with the appropriate neighboring Cu $3d$ orbitals.

The results of recent x-ray absorption[15] and electron-energy-loss[16] spectroscopy studies on the O $1s$ absorption edges in $Bi_2Sr_2CaCu_2O_8$ (Refs. 15 and 16) and $YBa_2Cu_3O_7$ (Ref. 16) single crystals exhibit polarization

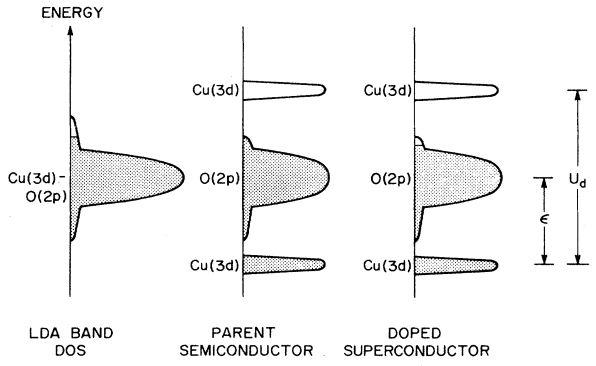

FIG. 1. Schematic representation of the LDA band-structure results for a prototype cuprate material ($CaCuO_2$) in comparison with a correlated picture based on an extended Hubbard-type model.

and orientation dependence that imply unoccupied O $2p$ hole states with either $\sigma(x,y)$ or $\pi(x,y)$ symmetry. The data suggest that the onset for $\pi(z)$ holes occurs at somewhat higher (~ 2 eV) excitation energies.

A simple procedure for estimating realistic O $2p$ bands in a situation where the Cu $3d$ electrons are localized by strong electron-electron interactions has been proposed by McMahan, Martin, and Satpathy (MMS) and applied to La_2CuO_4.[14] Their approach is based on the linear muffin-tin orbital (LMTO) method.[17] This scheme is similar in many respects to a minimum-basis linear-combination-of-atomic-orbitals (LCAO) approach. An unimportant technical difference is the fact that each valence orbital inside the muffin-tin (MT) spheres that surround each atom is represented by a numerical solution of Schrödinger's equation which tails off outside that sphere as a spherical bessel function. An important difference is that these basis-function tails, rather than extending into neighboring MT's themselves, are continued into these MT's by numerical functions computed within those spheres. This is done in such a manner that both value and slope continuity are maintained at each MT boundary.[17] In general, a basis function with a particular angular-momentum symmetry at one site [e.g., O $2p(x)$] will have components of all angular momenta within neighboring MT's [e.g., s, p (x,y,z), d $(xy, yz, zx, x^2-y^2, 3z^2-r^2)$, etc., within a Cu sphere]. The MMS procedure[14] consists of dropping the Cu d basis functions *in addition to* setting the d components of all other basis-function tails within the Cu spheres to zero. No attempt is made to restore wave-function continuity at the Cu spheres, and the infinite kinetic energy associated with the discontinuous basis functions is simply ignored.

The principal effect of the MMS procedure is to remove the strong $(pd\sigma)$ bonding interactions between the nearly degenerate Cu $d(x^2-y^2)$–O $\sigma(x,y)$ orbitals that produce the single half-filled antibonding subband at E_F. Of course, the less strongly coupled Cu d bands are also removed. As a result, the MMS scheme yields a model O $2p$ LDA band structure in which the overall La_2CuO_4 valence bandwidth is reduced from about 10.2 to 6.7 eV, while the Fermi level is lowered by ~ 1.4 eV. The uppermost O $2p$ bands in this model represent states that did not couple or were weakly coupled to the itinerant Cu $3d$ states. MMS find a major redistribution of these LDA states when Coulomb interactions are added in their many-body treatment, which then yields O $2p$ holes with $\sigma(x,y)$ symmetry.

The purpose of the present investigation is to provide an improved method for calculating the O $2p$ LDA bands in a cuprate compound where the Cu $3d$ electrons are assumed to be localized by correlation effects. In simplest terms, the procedure manipulates the linear augmented-plane-wave (LAPW) method[18] in a way that forces the calculated bands to be orthogonal to the Cu $3d$ states. Although similar in intent to the procedure of MMS,[14] the present approach represents a more clearly defined physical approximation and yields results which differ in important details from MMS. In particular, the predicted symmetry of the mobile O $2p$ holes [i.e., $\sigma(x,y)$] at low hole doping levels differs from the LDA results of MMS.

Because of its structural simplicity, the present investigation has focused on $Ca_{0.86}Sr_{0.14}CuO_2$, the recently synthesized[19] parent compound of the Bi-Sr-Ca-Cu-O and Tl-Ba-Ca-Cu-O families of superconductors. $Ca_{0.86}Sr_{0.14}CuO_2$ crystallizes with a simple-tetragonal structure (space group $P4/mmm$) with lattice parameters $a=3.86$ Å and $c=3.20$ Å, respectively. As shown in Fig. 2, this compound consists of flat CuO_2 planes which are separated by O-free layers that contain cation sites occupied by a $Ca_{0.86}Sr_{0.14}$ mixture. It is found[19] that partial Sr→Ca substitution is required to stabilize this simple-tetragonal phase, presumably to remove steric constraints of the pure Ca compound. Since $Ca_{0.86}Sr_{0.14}CuO_2$ contains the essential structural features of the more complicated cuprates, it represents an ideal model system for studying the effects of Cu $3d$ localization on the O $2p$ band states, simplifying both the details of the first-principles results as well as their tight-binding (TB) interpretation.

Since the Ca-Sr constituents are expected to be electronically inactive in $Ca_{0.86}Sr_{0.14}CuO_2$, the Sr alloying has been neglected in the present LAPW calculations that focus on the idealized parent compound, $CaCuO_2$. In this compound, the individual atom coordinates in the primitive unit cell correspond to Cu(0,0,0), O($\frac{1}{2}$,0,0), O(0,$\frac{1}{2}$,0), and Ca($\frac{1}{2}$,$\frac{1}{2}$,$\frac{1}{2}$), respectively, in units of (a,a,c). From its structural features, one can anticipate that $CaCuO_2$ will exhibit band dispersion that is more three-dimensional than its descendants, which have several "insulating" layers (such as BaO or SrO) separating the CuO_2 planes. The c-axis dispersion in $CaCuO_2$ manifests itself as molecular-orbital-type splittings of Cu—O bands in its descendants, which can have several adjacent Ca—CuO_2 layers per primitive cell. The three-dimensional banding in $CaCuO_2$ originates from direct interactions along c since these interplanar bond distances are comparable to those in the basal plane ($c/a \approx 0.83$). The only shorter bonds are the first nearest-neighbor (1 NN) Cu—O ($d=a/2=1.93$ Å) and O—O ($d=\sqrt{2}a/2=2.73$ Å) bond distances within the CuO_2 planes, which are $\sim 40\%$ and 15% smaller than those along the c axis.

The present implementation[18] of the LAPW method imposes no shape restrictions on either the charge density or the crystal potential. The exchange and correlation contributions to the potential have been included with

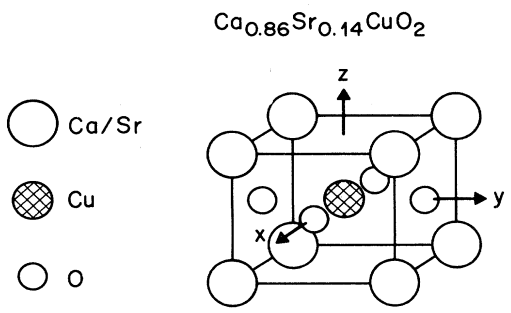

FIG. 2. Primitive unit cell for tetragonal $Ca_{0.86}Sr_{0.14}CuO_2$.

the use of the Wigner interpolation formula.[20] For the standard band-structure model, where all the electrons are itinerant, the self-consistent valence-electron charge density and potential have been calculated for bands arising from atomic Ca $4s^2$, Cu $3d^{10}4s$, and O $2s^22p^4$ states. The more tightly bound corelike states of each constituent are treated with the use of a frozen-core approximation.[18] The corresponding results for the band model in which the Cu $3d$ electrons are localized have been determined directly from the self-consistent potential for the itinerant Cu $3d$ LAPW calculation, using a "pseudopotential" trick that is described in detail below. The LDA is believed to provide an accurate representation of the charge density, and hence the self-consistent potential, even in a case where strong correlation effects render the LDA bands meaningless as excitation energies.

The LAPW basis size has been set to include all plane waves with energies up to a 12 Ry cutoff ($\sim$225 LAPW's). The spherical-harmonic expansion of the LAPW's within the individual nonoverlapping MT spheres [with radii $R(\mathrm{Cu})\approx 1.98$, $R(\mathrm{O})\approx 1.66$, and $R(\mathrm{Ca})\approx 2.80$ a.u., respectively] has included terms through $l_{\max}=8$. The charge density and potential have been expanded using $\sim$2700 plane waves (64 Ry) in the interstitial region and lattice-harmonic expansions ($l_{\max}=6$) within the MT's. The Brillouin-zone integrations have been carried out using a six-point **k** sample in the $\frac{1}{16}$ irreducible wedge.

The self-consistent LAPW band-structure results for $CaCuO_2$ with itinerant Cu $3d$ states are plotted along representative symmetry lines in the simple-tetragonal Brillouin zone in Fig. 3(a), where $X=(\pi/a,0,0)$, $M=(\pi/a,\pi/a,0)$, $Z=(0,0,\pi/c)$, $R=(\pi/a,0,\pi/c)$, and $A=(\pi/a,\pi/a,\pi/c)$, respectively. The band labels at M and A reflect Luehrmann's symmetry notation.[21] The eleven-band complex that spans the energy range from -7 to $+2$ eV originates from the Cu $3d$ and O $2p$ states and contains a total of 21 valence electrons. The results exhibit the characteristic feature of a cuprate superconductor parent compound in that the uppermost band, the Cu $d(x^2-y^2)$–O $\sigma(x,y)$ antibonding subband, is exactly half-filled. Consequently, it is not surprising that antiferromagnetism has been observed[22] in the actual Sr-substituted version of this compound.

Above E_F, the lower portions of the Cu $4s$ and Ca $3d$ bands overlap the antibonding $d(x^2-y^2)$—$\sigma(x,y)$ subband near Γ and A, respectively. The latter state has predominant Ca $d(xy)$ character. The pair of corelike O $2s$ levels fall well below the energy range shown in Fig. 3(a), extending from -16.2 to -17.7 eV below E_F.

As anticipated above, the LAPW band results for $CaCuO_2$ exhibit significant dispersion ($\sim$1–2 eV) along the c-axis direction (ΓZ) shown in Fig. 3(a). A comparison of the band profiles in the basal plane ($\Gamma XM\Gamma$) and top face ($ZRAZ$) of the Brillouin zone demonstrates that comparable c-axis dispersion extends throughout the entire zone.

The corresponding results shown in Fig. 3(b) are determined from a simple 17-parameter TB model that includes a basis of Cu $3d$ and O $2p$ orbitals. This TB scheme, whose parameters are listed under model C in Table I, provides a good qualitative description (rms error $\approx$0.3 eV) of the overall characteristics of the LAPW results shown in Fig. 3(a). This TB model includes 1 NN (planar) Cu $3d$—O $2p$, 1 NN (interplanar) Cu $3d$–Cu $3d$, and 1 NN (planar) and 2 NN (interplanar) O $2p$–O $2p$ interactions with the use of a modified two-center approximation.[23]. The details are discussed below. However, it is noted here that considerable complexity must be added to this TB model (in the form of more distant-neighbor

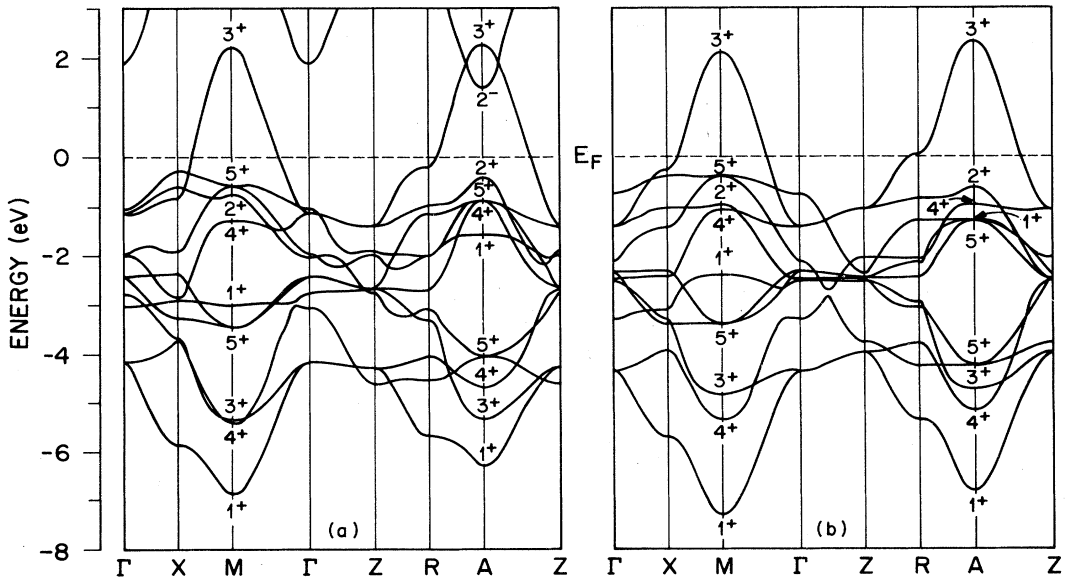

FIG. 3. LDA energy-band profiles for tetragonal $CaCuO_2$, as determined from (a) LAPW calculations and (b) a tight-binding fit (model C of Table I), respectively.

TABLE I. Tight-binding parameters (in eV) for $CaCuO_2$ with localized (model A) and itinerant (models B and C) Cu $3d$ states, as determined from fits to the LAPW results at symmetry points in Figs. 3(a) and 5(a), respectively. Integer subscripts denote 1 NN or 2 NN interactions over a distance d. Independent 1 NN $(pp\sigma)$-type parameters are defined in Fig. 7. The O $2p$ parameters are relaxed in model C but not B.

Parameter	d (Å)	Model A	Model B	Model C
$E_{p\sigma}$		−3.16	−3.16	−3.42
$E_{p\pi}$		−2.28	−2.28	−2.33
$(pp\sigma)_1$	2.73	0.87	0.87	0.85
$(pp\sigma)_1^s$	2.73	1.37	1.37	1.04
$(pp\sigma)_1^p$	2.73	0.57	0.57	0.61
$(pp\pi)_1$	2.73	−0.17	−0.17	−0.17
$(pp\sigma)_2$	3.20	0.41	0.41	0.44
$(pp\pi)_2$	3.20	−0.09	−0.09	−0.07
$E_{d(3z^2-r^2)}$			−2.69	−2.76
$E_{d(x^2-y^2)}$			−2.51	−2.20
$E_{d(xy)}$			−2.56	−2.51
$E_{d(xz,yz)}$			−2.42	−2.40
$(dd\sigma)_1$	3.20		−0.31	−0.32
$(dd\pi)_1$	3.20		0.03	0.02
$(dd\delta)_1$	3.20		0.00	−0.01
$(pd\sigma)_1$	1.93		−1.35	−1.39
$(pd\pi)_1$	1.93		0.72	0.72
$[(pp\sigma)_1^s(pp\sigma)_1^p]^{1/2}$	2.73	0.88	0.88	0.80
rms error		0.38	0.32	0.29

interactions as well as extra basis functions to represent unoccupied Ca and Cu bands) in order to improve the overall quality of the TB fit.

One can, in principle, utilize this TB model to simulate the situation where the Cu $3d$ electrons are localized simply by setting the Cu $3d$–O $2p$ and Cu $3d$–Cu $3d$ interactions to zero. However, experience has shown that this can often yield inaccurate results, especially for TB models that utilize an orthogonalized atomic-orbital basis[24] of the type considered here. These inaccuracies originate from the fact that TB parameters are "effective" matrix elements (of undefined basis functions) rather than actual matrix elements of a Hamiltonian, and this can severely limit their extrapolative properties in relatively complex, low-symmetry systems such as $CaCuO_2$. The procedure of dropping these matrix elements would not fully accomplish our intent, even in an *ab initio* LCAO approach. As noted above, the tails of neighboring O $2p$ orbitals can combine with each other around a Cu site to produce states with $3d$-type symmetry. This will allow a residual attractive Cu contribution to the O p-p interaction to remain, even after the explicit p-d interaction is set to zero, and will not properly represent the strongly correlated situation we wish to model.

These possible difficulties have been avoided by carrying out model LAPW calculations in which the Cu $3d$ electrons have been artificially localized by orthogonalizing the LAPW basis states to them. We believe that this gives the best possible one-electron representation of the O $2p$ manifold in the correlated situation sketched in Fig. 1, where the upper and lower Hubbard-type Cu $3d$ subbands are energetically removed from the range in which they can hybridize with this manifold. The results of such a calculation alter the valence bands in Fig. 3(a) by eliminating the five Cu $3d$ bands, leaving only the six O $2p$ bands. The dispersion characteristics of these remaining O $2p$ bands reflect hybridization with all but the Cu $3d$ states, though the influence of the localized Cu $3d$ electrons remains via their contribution to the crystal potential, and via a repulsive "pseudopotential" discussed below. As mentioned earlier, we believe that these model O $2p$ bands are most accurately generated by the standard LDA potential calculated with itinerant Cu $3d$ electrons.

Our technique for orthogonalizing the LAPW basis functions to the Cu $3d$ states exploits a characteristic property of this method in a novel way. It has been proved that valence-band LAPW basis functions are orthogonal to core states, but this proof involves the requirement that the core states are identically zero beyond the MT boundaries.[17] This condition is poorly satisfied for shallow core states, and we have discussed the fact that it is sometimes necessary to adjust the energies E_l at which the MT radial basis functions are evaluated so as to optimize the desired orthogonalization.[18] Failure to do so can result in the appearance of "ghost" bands, poorly converged, shallow, corelike states falling within the valence-band energy range, typically at isolated $\mathbf{k}$ points. In the course of systematically exploring this effect, we have observed that the LAPW basis set can be switched from one which represents bands of principal quantum number n (for a particular atom and l) to one which corresponds to principal quantum number $n+1$. Our normal procedure is to set the E_l for each atom and l so that it maintains the same energy relationship to the spherically averaged potential in the core region as does the corresponding atomic valence level. This systematically places the maximum accuracy for the corresponding piece of the LAPW basis function in the bands where it has the largest weight.[18]

The process of switching Cu $3d$ out of the LAPW basis for $CaCuO_2$ is illustrated in Fig. 4. The cross-hatched curve depicts the variation of the Cu d-band energies at Γ as E_d is increased from its reference[18] or atomic value to one where $E_d - E_F \approx 20$ eV. As expected,[17] the band energies are initially very stable with respect to changes in E_d, but they then increase rapidly as the effective Cu d principal quantum number shifts from $n=3$ to $n=4$. Analogous results are obtained at other $\mathbf{k}$ values, though Γ is simplified because there is no Cu d–O p mixing. For $E_d - E_F \approx 20$ eV, where our calculation has been carried out, this procedure produces moderately converged bands of predominant Cu $4d$ character well up in the conduction-band energy range, which we ignore. These mix only weakly with the remaining O $2p$ bands, whose energies are essentially independent of E_d once it is above ~ 16 eV. Physically, it is clear that the resulting band states are poor solutions to the Schrödinger equation for the crystal potential in the energy range of the O $2p$ manifold. They correspond in fact to accurate solutions for a modified potential in which a repulsive d pseudopotential

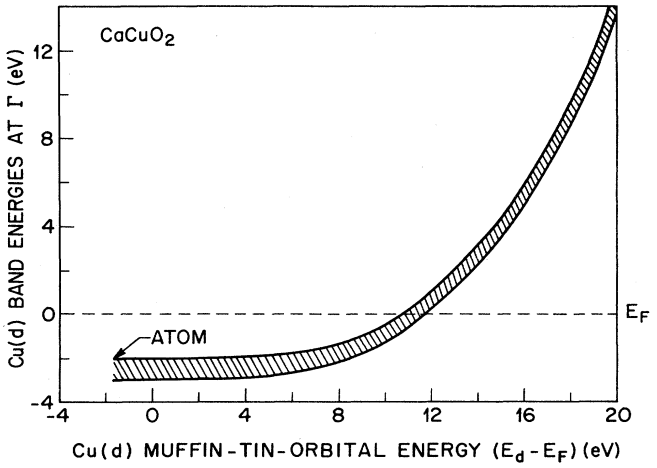

FIG. 4. Variation of the Cu d-band energies at Γ (which span the cross-hatched energy range) as a function of E_d, the $l=2$ muffin-tin-orbital energy inside the Cu spheres.

has been added to each Cu site.

The application of this procedure to the $CaCuO_2$ system with "localized" Cu $3d$ states produces the model LAPW O $2p$ bands that are shown in Fig. 5(a). Although the energies of these localized Cu $3d$ states are undetermined by this procedure, the TB results of model C in Table I indicate that they fall in the energy range of -2.2 to -2.8 eV, while the unoccupied $4d$ bands have been shifted to an energy ~ 14 eV above E_F (Fig. 4). The six remaining O $2p$ bands are essentially decoupled into noninteracting $\sigma(x,y)$-$\pi(x,y)$ (solid lines) and $\pi(z)$ (dashed lines) subbands. The band energies of those O $2p$ states that do not hybridize with the Cu $3d$ states (i.e., M_{2+}, A_{2+} as well as all the states at Γ and Z) are unchanged from those shown in Fig. 3(a).

A significant feature of the O $2p$ bands in Fig. 5(a) is the fact that the uppermost valence-band states at M and A retain the same M_{3+}, A_{3+} symmetry as found for the itinerant Cu $3d$ limit [Fig. 3(a)], though their energies are lowered so they nearly coincide with the original Fermi level. Their energy position provides additional evidence that the model accomplishes our intent: The energy at which the first hole can be added, a quantity which is accurately given by density functional theory,[25] is preserved in going from the metallic to the model correlated state. According to these model LAPW results, any additional holes that are introduced into the CuO_2 planes will initially deplete $\sigma(x,y)$ bands near the vertical edges (i.e., along the MA line) of the simple-tetragonal Brillouin zone. The $\pi(x,y)$ and $\pi(z)$ will contribute only at higher-doping levels.

The model LDA results shown in Fig. 5(a) differ substantially from those of MMS,[14] where the analogous La_2CuO_4 Cu $d(x^2-y^2)$-O $\sigma(x,y)$ band drops to a significantly lower (~ 3 eV overall) energy. Their elimination of the Cu d states within the Cu atomic spheres without regard to the continuity of the O $2p$ wavefunction overlap into these spheres causes the energies of those O $2p$ bands that interact with the Cu $3d$ states to be artificially lowered. The "boundary condition" imposed by our requirement that these band states be orthogonal to the localized Cu $3d$ electrons is absent in the MMS approach. On the other hand, the present LAPW model for localized Cu $3d$ states allows these O $2p$ states to continuously penetrate the Cu MT's, but forces them to have a $4d$-like node near the sphere boundary, thereby increasing their kinetic energy.

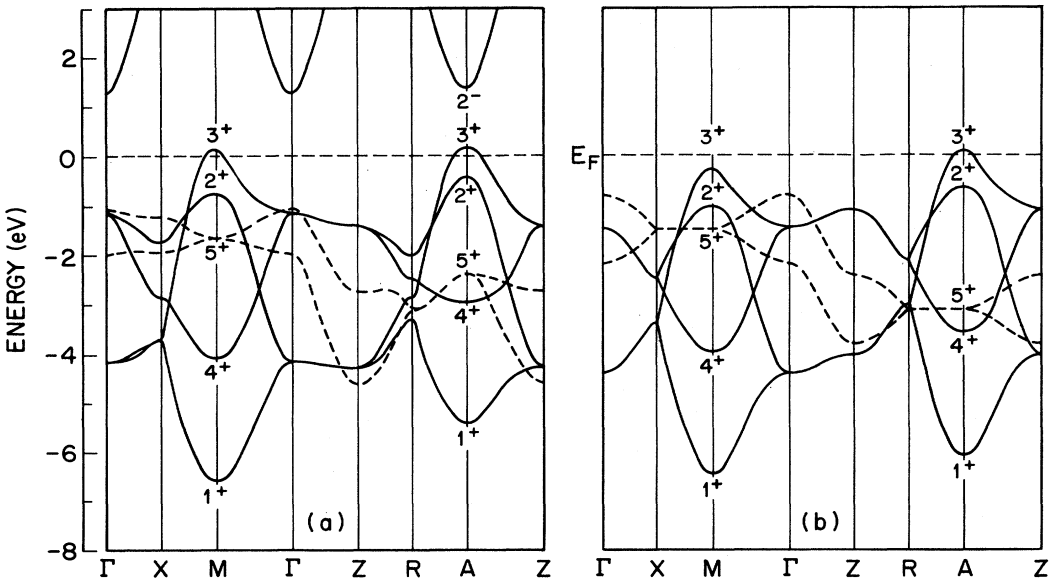

FIG. 5. Model LDA energy-band results for $CaCuO_2$ with localized Cu($3d$) electrons, as determined from (a) LAPW calculations and (b) a tight-binding fit (model A of Table I), respectively. The dashed curves denote the $\pi(z)$ subbands.

The nodal structure of our mobile O $2p$ hole wave functions is shown in Fig. 6, through contour plots of the sum of the charge densities of the M_{3+} and A_{3+} states. A small residue of $d(x^2-y^2)$ charge representing the inner peak of the weakly admixed Cu $4d$ state can be seen. Comparing Figs. 6(a) and 6(b) shows the O $2p$ charge to be essentially symmetric about the Cu-O axis. The O $2p$ charge in these states is quite compact, despite the nominal -2 charge state of the O ions. In fact, a plot of the charge density along the Cu-O axis is essentially indistinguishable from that of the scaled *neutral* atomic O $2p$ charge density. The compactness of our effective mobile O $2p$ hole state is apparently a result of the combined confining tendencies of the Madelung potential and the Cu repulsive d "pseudopotential."

The LAPW results at the six symmetry points in Fig. 5(a) have been fit by means of an eight-parameter TB model involving a six-orbital O $2p$ basis. The resulting bands, which are derived from the parameters listed under model A in Table I, are shown in Fig. 5(b). While the rms error in the fit is about 0.4 eV, the TB results mimic adequately the general characteristic features of the LAPW results.

In order to optimize the accuracy of this TB fit with a minimal number of parameters, it is necessary to modify the usual two-center approximation to the Slater-Koster[23] energy integrals $E_{\alpha,\beta}(\mathbf{r}_n)$ that describe the interaction between orbitals α and β which are separated by $\mathbf{r}_n$. A detailed analysis of the LAPW results shows that these modifications are especially important in treating 1 NN interactions among the $\sigma(x,y)$ and $\pi(x,y)$ orbitals. The key elements of this modified two-center treatment of these energy parameters are illustrated schematically in Fig. 7. As shown, this approach maintains the distinction between the independent energy integrals $E_{x,y}(\frac{1}{2}\frac{1}{2}0)$, $E_{y,x}(\frac{1}{2}\frac{1}{2}0)$, and $E_{x,x}(\frac{1}{2}\frac{1}{2}0)$ by introducing three $(pp\sigma)$-type parameters $[(pp\sigma)_1^s$, $(pp\sigma)_1^p$, and $(pp\sigma)_1$, respectively] to describe the 1 NN interactions between $\sigma(x,y)$ orbitals [Fig. 7(a)], $\pi(x,y)$ orbitals [Fig. 7(b)], and $\sigma(x,y)-\pi(x,y)$ [Fig. 7(c)] combinations. In all cases [including interactions between $\pi(z)$ orbitals], the corresponding π-type interactions are represented by means of a single $(pp\pi)_1$ parameter.

The importance of this modified two-center treatment is reflected in the TB parameters which are listed under model A in Table I. According to these results, the energy integrals $E_{x,y}(\frac{1}{2}\frac{1}{2}0)$ and $E_{y,x}(\frac{1}{2}\frac{1}{2}0)$, which are equal ($\approx$0.52 eV) in the standard two-center approximation, have the optimal (fitted) values of 0.77 eV and 0.37 eV, respectively. The effect of these differences on the TB bands is discussed below. The hybrid parameter, $(pp\sigma)_1$, is accurately approximated by the geometric mean of the $\sigma(x,y)$ and $\pi(x,y)$ parameters, $[(pp\sigma)_1^s(pp\sigma)_1^p]^{1/2}$. These anisotropy effects become less important in the 2 NN parameters (i.e., those representing the c-axis dispersion)

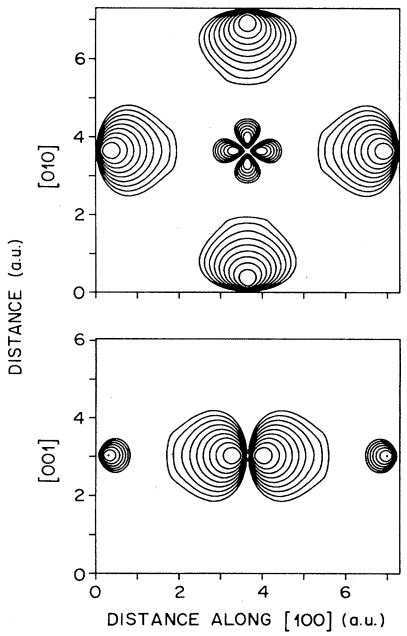

FIG. 6. Charge-density contours on the central (a) (001) and (b) (100) planes of the $CaCuO_2$ structure for the M_{3+}, A_{3+} states in Fig. 5(a). The diminished $d(x^2-y^2)$ contours at the (a) center and (b) edge of the plots reflect the slight Cu $4d$ admixture with the predominant O $\sigma(x,y)$ component. The outermost contour values are 0.01 electron/a.u. and the contour increments are spaced logarithmically, six to the decade (0.01, 0.0147, 0.0215, etc.).

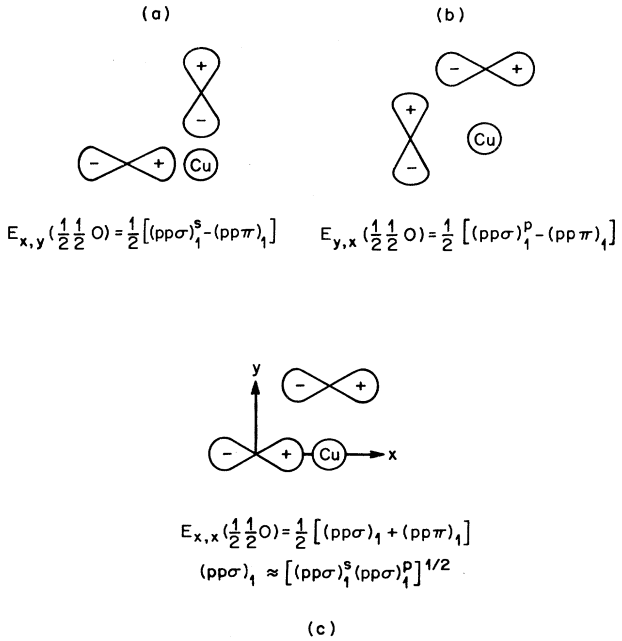

FIG. 7. Pictorial representation of the Slater-Koster nearest-neighbor O $2p$–O $2p$ energy integrals (a) $E_{x,y}(\frac{1}{2}\frac{1}{2}0)$, (b) $E_{y,x}(\frac{1}{2}\frac{1}{2}0)$, and (c) $E_{x,x}(\frac{1}{2}\frac{1}{2}0)$, including their decomposition in terms of a modified two-center approximation.

since they are reduced from the 1 NN values by about a factor of 2.

In order to better understand the model O $2p$ band-structure results in Fig. 5, it is useful to analyze the phase patterns which are imposed by translational symmetry on the bonding and antibonding combinations of the $\sigma(x,y)$ and $\pi(x,y)$ orbitals for wave vectors along the MA line of the Brillouin zone. These are illustrated in Fig. 8. Unlike the usual picture where states with same symmetry interact to form bonding and antibonding combinations, the bonding and antibonding states within the CuO_2 planes have *different* symmetry. In the case of the $\sigma(x,y)$ orbitals, the bonding and antibonding combinations have M_{1+} and M_{3+} symmetry, respectively, whereas the bonding and antibonding configurations of $\pi(x,y)$ orbitals have M_{4+} and M_{2+} symmetry, respectively.

By extending the phase patterns of the various $\sigma(x,y)$ and $\pi(x,y)$ bonding and antibonding states so as to fully surround a Cu site, one can deduce visually the symmetry of Cu-type orbitals that hybridize with these O $2p$ combinations. For example, it is obvious that the M_{1+} state interacts with Cu s or $d(3z^2-r^2)$ orbitals, M_{3+} with $d(x^2-y^2)$ orbitals, M_{4+} with $d(xy)$ orbitals, while M_{2+} is orthogonal all Cu $3d$ states. In addition, one can also understand why O $2p$ – Cu $4p$ interactions vanish at the M and A points.

This analysis permits us to describe more fully the relationship between the TB parameters in Table I and the O $2p$ band results of Fig. 5. For example, by neglecting the difference between the $E_{p\sigma}-E_{p\pi}$ TB orbital energies in Table I, the TB estimate of the $\sigma(x,y)-\pi(x,y)$ bandwidth (solid lines) at Γ or Z, namely $8E_{x,x}(\frac{1}{2}\frac{1}{2}0)=4[(pp\sigma)_1+(pp\pi)_1]$, is about 2.8 eV, in agreement with Fig. 5. Neglecting the $(pp\sigma)_1^s-(pp\sigma)_1^p$ anisotropy, the application of the standard two-center approximation yields identical energy separations ($\sim$4.2 eV) between the M_{3+},M_{1+} and M_{2+},M_{4+} bonding-antibonding pairs, whereas the modified two-center treatment properly describes the fact that the M_{3+},M_{1+} separation $(8E_{x,y}(\frac{1}{2}\frac{1}{2}0)=4[(pp\sigma)_1^s-(pp\pi)_1]\approx 6.2$ eV) is about twice as large as that exhibited by the M_{2+},M_{4+} $(8E_{y,x}(\frac{1}{2}\frac{1}{2}0)=4[(pp\sigma)_1^p-(pp\pi)_1]\approx 3.0$ eV) subbands.

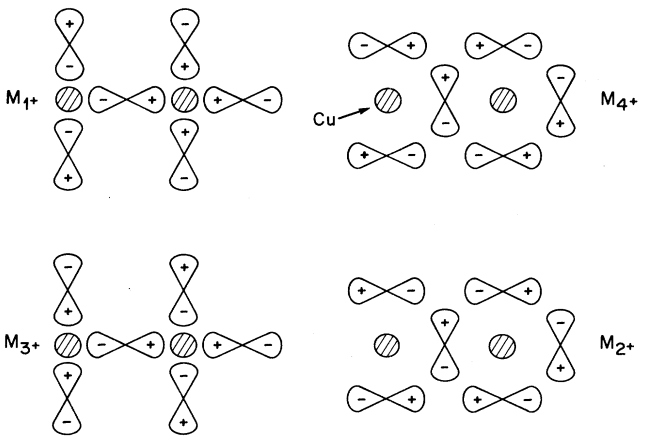

FIG. 8. Phase patterns depicting the bonding-antibonding symmetry of the $\sigma(x,y)$ (M_{1+}/M_{3+}) and $\pi(x,y)$ (M_{4+}/M_{2+}) O $2p$-type orbitals for wave vectors along the MA line of the Brillouin zone.

It is important to note that this $(pp\sigma)_1^s-(pp\sigma)_1^p$ anisotropy is also present in the band-structure results for the body-centered-tetragonal (bct) cuprates such as La_2CuO_4, though in a less obvious way. This ambiguity arises from the fact that the corresponding [110] zone-boundary states for the $I4/mmm$ space group have lower point-group symmetry.[21] As a result, the corresponding M_{1+},M_{4+} states in Fig. 5 share one symmetry (X_{1+}) while the M_{2+},M_{3+} pair shares another (X_{2+}) in the bct materials. The resulting ambiguity can lead to the incorrect identification of bonding-antibonding pairs in a TB fit to the bct bands when the standard two-center approximation is employed.

Efforts to improve the quality of the TB fit shown in Fig. 5 reveal that a significantly more complicated model is required. For example, while 3 NN O $2p$–O $2p$ interactions will remove the accidental degeneracies at X and R in Fig. 5(b), the sign of the LAPW splittings in Fig. 5(a) alternate between X and R in such a way that the net improvement in accuracy is minimal. The source of these difficulties is evident from an examination of the LAPW wave functions. This reveals significant weight ($\approx$0.05–0.17) resulting from the admixture of the O $2p$ bands with unoccupied Cu $4s$-$4p$ and Ca $4s$-$4p$-$3d$ states. Thus, an improved TB treatment would require an expanded TB basis which includes these orbitals as well as more distant neighbor O $2p$–O $2p$ interactions.

A well-known problem of TB models is the fact that the fitting parameters are not generally unique. This problem becomes more serious when the parametrization includes orbital-overlap effects[24] or in cases where the parameter set is expanded to achieve a highly accurate fit to first-principles band-structure results. Under these circumstances, the TB parameters lose the underlying physical significance that is an important asset of the TB approach. These effects are minimized in the present analysis because of the relative simplicity of the $CaCuO_2$ structure. This is evident from a comparison between the O $2p$ parameters in model A and model C of Table I. With two exceptions, the parameter changes are less that 0.1 eV when unrestricted fits are carried out on the results in Figs. 5(a) and 3(a), respectively.

Additional insight regarding the significance of these differences is provided by the model B results. In this case, the O $2p$ parameters from model A have been frozen and only the Cu $3d$ and Cu $3d$–O $2p$ subset has been varied. This yields a modestly higher ($\sim$0.03 eV) rms error than that obtained in model C, where all parameters have been varied. Comparing the model B and model C parameters, one finds that correlated variations in $E_{p\sigma}$, $(pp\sigma)_1^s$, and $E_{d(x^2-y^2)}$ produce minimal changes in the overall rms errors, which suggests that these parameters are not well determined by the standard $CaCuO_2$ bands, despite the relatively simple crystal structure of this material.

Of course, similar ambiguities manifest themselves in other attempts[14,26,27] to extract TB parameters for use in studies involving Hubbard-type Hamiltonians. Estimates of the 1 NN O $2p$–O $2p$ hopping integral $E_{x,y}(\frac{1}{2}\frac{1}{2}0)$ or $E_{y,x}(\frac{1}{2},\frac{1}{2}0)$, which are usually denoted by t_{pp}, vary in the range from 0.65 eV (Refs. 14 and 27), 0.6 eV (Ref. 28), 0.53 eV (Ref. 9), 0.5 eV (Ref. 29), 0.33 eV (Ref. 26), to 0.1 eV (Ref. 30). The present TB model, which distinguishes between the $\sigma(x,y)$ and $\pi(x,y)$ interactions, yields t_{pp} values of $E_{x,y}(\frac{1}{2}\frac{1}{2}0)\approx 0.77$ eV and $E_{y,x}(\frac{1}{2}\frac{1}{2}0)\approx 0.37$ eV, respectively. Neglecting this anisotropy, the present results imply a (geometrical) mean value of $t_{pp}\approx 0.52$ eV, which is close to the average of the values quoted above. This suggests that the use of a modified two-center approximation may be an important ingredient for obtaining an accurate TB description of the cuprate band structures in the high-T_c superconductors and their parent compounds.

TB model B, which represents a simultaneous fit to our itinerant Cu $3d$ or "mean-field" bands[8] and our model localized Cu $3d$ results, eliminates these ambiguities. In an earlier discussion, we pointed out that an attempt to describe the localized limit simply to zeroing the Cu—Cu and Cu—O matrix elements in fit C would be inaccurate because of the "effective" character of the TB matrix elements. While the parameters of model B are still effective matrix elements between undefined states, they now accomplish this purpose. Since model B can represent the two limits of itinerant and localized Cu $3d$ electrons with comparable accuracy, we believe it represents an accurate starting point for many-body calculations intended to probe the real situation, which is undoubtedly intermediate between these extremes.

To summarize, we have proposed a simple procedure for calculating the O $2p$ bands in a cuprate compound with localized Cu $3d$ electrons within the framework of the LAPW method. The results predict that the chemically induced holes occur initially in the O $2p$ $\sigma(x,y)$ subbands, with the $\pi(x,y)$ and $\pi(z)$ states contributing only at higher-doping levels. A TB fit to the LAPW results for itinerant and localized Cu $3d$ states yields O $2p$ parameters that describe both limits. An important feature of this TB model is the use of a modified two-center approximation to accurately describe 1 NN O $2p$–O $2p$ interactions.

ACKNOWLEDGMENTS

We are pleased to acknowledge informative conversations with R. M. Martin and A. K. McMahon concerning technical aspects of their LMTO calculations for La_2CuO_4.

[1]J. G. Bednorz and K. A. Müller, Z. Phys. B **64**, 189 (1986).
[2]L. F. Mattheiss, Phys. Rev. Lett. **58**, 1028 (1987).
[3]J. Yu, A. J. Freeman, and J.-H. Xu, Phys. Rev. Lett. **58**, 1035 (1987).
[4]T. C. Leung, X. W. Wang, and B. N. Harmon, Phys. Rev. B **37**, 384 (1988).
[5]D. Vaknin *et al.*, Phys. Rev. Lett. **58**, 2802 (1987); T. Freltoft *et al.*, Phys. Rev. B **36**, 826 (1987).
[6]For a review of the early studies, see G. Wendin, J. Phys. (Paris) Colloq. C9 **48**, 1157 (1987).
[7]P. W. Anderson, Science **235**, 1196 (1987).
[8]V. J. Emery, Phys. Rev. Lett. **58**, 2794 (1987).
[9]E. B. Stechel and D. R. Jennison, Phys. Rev. B **38**, 4632 (1988).
[10]Y. Guo, J.-M. Langlois, and W. A. Goddard III, Science **239**, 896 (1988).
[11]R. J. Birgeneau, M. A. Kastner, and A. Aharony, Z. Phys. B **71**, 57 (1988).
[12]F. Adrian, Phys. Rev. B **37**, 2326 (1988).
[13]K. H. Johnson *et al.*, Physica C **153-155**, 1165 (1988).
[14]A. K. McMahon, R. M. Martin, and S. Satpathy, Phys. Rev. B **38**, 6650 (1988).
[15]F. J. Himpsel, G. V. Chandrashekhar, A. B. McLean, and M. W. Shafer, Phys. Rev. B **38**, 11 946 (1988).
[16]N. Nücker, H. Romberg, X. X. Xi, J. Fink, B. Gegenheimer, and Z. X. Zhao, Phys. Rev. B **39**, 6619 (1989).
[17]O. K. Andersen, Phys. Rev. B **12**, 3060 (1975).
[18]L. F. Mattheiss and D. R. Hamann, Phys. Rev. B **33**, 823 (1986).
[19]T. Siegrist, S. M. Zahurak, D. W. Murphy, and R. S. Roth, Nature (London) **334**, 231 (1988).
[20]E. Wigner, Phys. Rev. **46**, 1002 (1934).
[21]A. W. Luehrmann, Adv. Phys. **17**, 1 (1968).
[22]D. Vaknin, E. Caignol, P. K. Davies, J. E. Fischer, D. C. Johnston, and D. P. Goshorn, Phys. Rev. B **39**, 9122 (1989).
[23]J. C. Slater and G. F. Koster, Phys. Rev. **94**, 1498 (1954).
[24]L. F. Mattheiss, Phys. Rev. B **2**, 3918 (1970).
[25]L. J. Sham and W. Kohn, Phys. Rev. **145**, 561 (1966).
[26]F. Mila, Phys. Rev. B **38**, 11358 (1988).
[27]M. S. Hybertsen, M. Schlüter, and N. E. Christensen, Phys. Rev. B **39**, 9028 (1989).
[28]K. T. Park, K. Terakura, T. Oguchi, A. Yanase, and M. Ikeda, Tech. Rep. ISSP, Ser. A, No. 1960, 1 (1988).
[29]W. Weber, Phys. Rev. Lett. **58**, 1371 (1987).
[30]M. J. DeWeert, D. A. Papaconstantopoulos, and W. E. Pickett, Phys. Rev. B **39**, 4235 (1989).